Early Effector Cells Survive The Contraction Phase In Malaria Infection And Generate Both Central And Effector Memory T Cells

By: **Michael M. Opata**, Victor H. Carpio, Samad A. Ibitokou, Brian E. Dillon, Joshua M. Obiero, & Robin Stephens

Abstract

CD4 T cells orchestrate immunity against blood-stage malaria. However, a major challenge in designing vaccines to the disease is poor understanding of the requirements for the generation of protective memory T cells (Tmem) from responding effector T cells (Teff) in chronic parasite infection. In this study, we use a transgenic mouse model with T cells specific for the merozoite surface protein (MSP)-1 of Plasmodium chabaudi to show that activated T cells generate three distinct Teff subsets with progressive activation phenotypes. The earliest observed Teff subsets (CD127−CD62LhiCD27+) are less divided than CD62Llo Teff and express memory genes. Intermediate (CD62LloCD27+) effector subsets include the most multicytokine-producing T cells, whereas fully activated (CD62LloCD27−) late effector cells have a terminal Teff phenotype (PD-1+, Fashi, AnnexinV+). We show that although IL-2 promotes expansion, it actually slows terminal effector differentiation. Using adoptive transfer, we show that only early Teff survive the contraction phase and generate the terminal late Teff subsets, whereas in uninfected recipients, they become both central and effector Tmem. Furthermore, we show that progression toward full Teff activation is promoted by increased duration of infection, which in the long-term promotes Tem differentiation.

Michael M. Opata, Victor H. Carpio, Samad A. Ibitokou, Brian E. Dillon, Joshua M. Obiero, Robin Stephens; Early Effector Cells Survive the Contraction Phase in Malaria Infection and Generate Both Central and Effector Memory T Cells. J Immunol 1 June 2015; 194 (11): 5346–5354. Publisher version of record available at: https://doi.org/10.4049/jimmunol.1403216

Early Effector Cells Survive the Contraction Phase in Malaria Infection and Generate Both Central and Effector Memory T Cells

Michael M. Opata,* Victor H. Carpio,*,† Samad A. Ibitokou,* Brian E. Dillon,* Joshua M. Obiero,* and Robin Stephens*,†

CD4 T cells orchestrate immunity against blood-stage malaria. However, a major challenge in designing vaccines to the disease is poor understanding of the requirements for the generation of protective memory T cells (Tmem) from responding effector T cells (Teff) in chronic parasite infection. In this study, we use a transgenic mouse model with T cells specific for the merozoite surface protein (MSP)-1 of *Plasmodium chabaudi* to show that activated T cells generate three distinct Teff subsets with progressive activation phenotypes. The earliest observed Teff subsets ($CD127^{-}CD62L^{hi}CD27^{+}$) are less divided than $CD62L^{lo}$ Teff and express memory genes. Intermediate ($CD62L^{lo}CD27^{+}$) effector subsets include the most multicytokine-producing T cells, whereas fully activated ($CD62L^{lo}CD27^{-}$) late effector cells have a terminal Teff phenotype ($PD\text{-}1^{+}$, Fas^{hi}, $AnnexinV^{+}$). We show that although IL-2 promotes expansion, it actually slows terminal effector differentiation. Using adoptive transfer, we show that only early Teff survive the contraction phase and generate the terminal late Teff subsets, whereas in uninfected recipients, they become both central and effector Tmem. Furthermore, we show that progression toward full Teff activation is promoted by increased duration of infection, which in the long-term promotes Tem differentiation. Therefore, we have defined markers of progressive activation of CD4 Teff at the peak of malaria infection, including a subset that survives the contraction phase to make Tmem, and show that Ag and cytokine levels during CD4 T cell expansion influence the proportion of activated cells that can survive contraction and generate memory in malaria infection. *The Journal of Immunology*, **2015, 194: 5346–5354.**

Malaria infection induces severe immunopathology with significant long-term global health and economic consequences (1). People in endemic areas quickly become resistant to severe disease but develop immunity only after repeated and chronic infections over many years, with prevalence of parasitemia falling off by adulthood by ~70% (2–4). During the symptomatic erythrocytic stage of *Plasmodium* infection, both CD4 T and B cells are essential for production of Ab for clearance of parasites, and memory cells are essential throughout life to recognize cumulative parasite diversity (5, 6). Th1 cells are also critical to activate phagocytes by enhancing parasite killing (7) and regulating immunopathology in both mice and humans by production of IL-10, IL-27, and TGF-β (8, 9). Therefore, CD4 T cells are essential for protection from lethal disease (10), and study of the CD4 T cell response to the pathological blood-stage of parasitemia will lead to development of protective vaccine strategies.

We have studied the immune response to *Plasmodium chabaudi*, a rodent model of chronic malaria infection (11), with the goal of understanding the activation and development of CD4 T cells in malaria parasite infection. As in other chronic parasitic infections (12–14), chronic *P. chabaudi* infection maintains protection to reinfection (15). Effector memory T cells (Tem) (12, 16–19) and effector T cells (Teff) (13, 14) have been implicated in this phenomenon, called premunition, but the cellular mechanisms of maintaining protection, by continuous effector generation or maintenance of Tem, and avoiding full exhaustion, remain unclear. Although PD1 expression has been identified during infection (17, 20, 21), it is clear that functional effector cells are generated and that some functional memory cells emerge (16, 17). Therefore, we investigated CD4 T cell memory in *P. chabaudi* and found a reduction of classical memory T cell (Tmem; $CD44^{hi}$ $CD127^{hi}$) in chronic infection, suggesting that traditional central memory cells did not provide the improved protection. Importantly, the majority of $CD44^{hi}$ Tmem in the chronic infection did not survive by homeostatic proliferation, did not proliferate quickly to secondary infection, and had the phenotype of Tem (22). We also studied B cell memory and found only a small effect of chronic infection (23), suggesting that Th cells may induce this effect. We showed the important role of CD4 memory cells in protection by a transfer of chronically stimulated, $CD44^{hi}CD25^{-}$ $CD4^{+}$ T cells, which protect better than resting Tmem (17). Subsequently, looking at MSP-1–specific B5 TCR transgenic (Tg) T cells (10), we identified an increase in $CD44^{hi}CD62L^{lo}IFN\gamma^{+}$ $TNF^{+}IL\text{-}2^{-}$ T cells at memory time points in chronic infection compared with animals with a treated infection (17). However,

*Division of Infectious Diseases, Department of Internal Medicine, University of Texas Medical Branch, Galveston, TX 77555; and †Department of Microbiology and Immunology, University of Texas Medical Branch, Galveston, TX 77555

Received for publication December 24, 2014. Accepted for publication March 18, 2015.

This work was supported by National Institute of Allergy and Infectious Diseases Grants R01AI08995304 (to R.S., M.M.O., and S.A.I.), R01AI08995304S1 (to V.H.C.), and T32AI7536-15 (to M.M.O.).

Address correspondence and reprint requests to Dr. Robin Stephens, Department of Internal Medicine, Division of Infectious Diseases, University of Texas Medical Branch, 301 University Boulevard, Galveston, TX 77555-0435. E-mail address: rostephe@utmb.edu

The online version of this article contains supplemental material.

Abbreviations used in this article: CD62L, L-selectin; CQ, chloroquine; CT, threshold cycle; MQ, mefloquine hydrochloride; MSP-1, merozoite surface protein-1; p.i., postinfection; Tcm, central memory T cell; Teff, effector T cell; $Teff^{Early}$, early Teff; $Teff^{Int}$, intermediate Teff; $Teff^{Late}$, late Teff; Tem, effector memory T cell; Tfh, T follicular helper; Tg, transgenic; Tmem, memory T cell.

there was no decrease in the number of Tem ($CD44^{hi}CD127^{hi}CD62L^{lo}$) in the absence of infection for 1 mo, suggesting that Tem cytokine potential, or their ability to generate Teff and not necessarily their survival, depends on persistent infection. Furthermore, we showed that protective Tem were derived from central memory T cells (Tcm) in chronic infection (17), suggesting that they are not simply derived from long-lived Teff. These data led us to hypothesize that Tem survive after persistent infection clears and provide sentinel activity for some time, even after clearance of infection. This idea has been well supported by research on resident Tem (24). Therefore, the question becomes how to drive the generation of cytokine-producing Tem for protective vaccination protocols for chronic infection.

Recent evidence suggests that CD4 Tmem differentiation is determined in the earliest stages of activation and that pre-Tcm and Tem can be detected concurrently with effector differentiation (25–27). This important work suggests that, to understand Tem differentiation and the potential to make protective Tem against malaria by vaccination, we must follow effector activation from the beginning to find the precursors of long-lived Tem (reviewed in Ref. 28). We hypothesized that Tem were either generated from early (26, 29) or late effector cells (25, 30). However, it was not possible to identify both of these Teff subsets in our BALB/c MSP1–specific B5 TCR Tg adoptive transfer system because the only marker of CD4 terminal Teff described to date, Ly6C (27), does not stain CD4 cells in BALB/c. Therefore, we identified new markers of progressive activation of CD4 effector cells for the purpose of determining the derivation of CD4 Tmem in *P. chabaudi* malaria.

The markers CD127, L-selectin (CD62L), and CD27 are well described molecules downregulated upon activation (17, 31, 32), each with different kinetics. Therefore, we tested whether these facile surface markers, that we previously used to define progressively differentiated CD4 Tmem subsets (17), provide a good marker panel to distinguish Teff phases along the spectrum of activation. In these studies, we show progressive activation of CD4 Teff from early ($Teff^{Early}$; $CD127^{-}CD62L^{hi}$), which express high levels of antiapoptotic genes, to intermediate effector cells ($Teff^{Int}$; $CD127^{-}CD62L^{lo}CD27^{+}$), that make more cytokines to fully activated late Teff ($Teff^{Late}$; $CD127^{-}CD62L^{lo}CD27^{-}$), which are terminally differentiated. By adoptive transfer at the peak of infection, we define a linear progression of activation phenotypes and confirm their ability to make terminally differentiated Teff and survive the contraction phase to generate Tmem, as suggested by previous studies on early effector cells (25–27). Furthermore, we show that only the early effector cell subset generates both Tcm and Tem in the long term and that the ratio of these is regulated by the duration of Ag exposure. These data will inform future studies on the differentiation pathway of CD4 Tem in malaria infection, which are necessary to understand how to develop vaccine strategies that will induce protective immunity.

Materials and Methods

Mice, parasites, and in vivo experiments

Thy1.1 BALB/cByJ were backcrossed to BALB/cJ (N4; The Jackson Laboratory, Bar Harbor, ME) and maintained in our specific pathogen-free animal facility with ad libitum access to food and water. B5 TCR Tg mice, a gift from J. Langhorne (MRC National Institute for Medical Research, London, UK), were generated as previously described (10) and backcrossed to BALB/cJ (N4-9). The B5 TCR recognizes MSP1 (1157–1171, ISVLKSRLLKRKKYI/I-E^{d}); B5 TCR Tg mice were typed using primers Vα2, 5′-gaacgttccagattccatgg-3′ and 5′-atggacaagatcctgacagcatcg-3′, and Vβ8.1, 5′-cagagaccctcaggcggctgctcagg-3′ and 5′-atgggctccaggctgttctttgtgg-ttttgattc-3′. *Ifng*/Thy1.1 knockin mice on a C57BL/6 background (25) were a gift from C. Weaver (University of Alabama, Birmingham, AL). Mice 6–12 wk old were infected with 10^{5} *Plasmodium chabaudi chabaudi* (AS)–infected erythrocytes i.p. Parasites are counted in thin blood smears stained with Giemsa (Sigma-Aldrich, St. Louis, MO) by light microscopy. In some experiments, mice were treated with 4 mg/kg mefloquine hydrochloride (MQ) antimalarial drug by oral gavage for 3 d starting day 3 or 5 or chloroquine (CQ) on days 30–34 postinfection (p.i.). Anti–IL-2 (mixture of clones S4B6 and JES6-1) or rat IgG2a control (clone 2A3; BioXCell, West Lebanon, NH) (0.25 mg of each Ab/mouse) were administered in saline i.p. every other day starting on day 1 p.i.

All experiments were carried out in accordance with the protocol approved by the University of Texas Medical Branch Institutional Animal Care and Use Committee.

Flow cytometry

Single-cell suspensions from spleens were made in HEPES-buffered HBSS (Life Technologies), incubated in RBC lysis buffer (eBioscience, San Diego, CA), and stained in PBS supplemented with 2% FBS (Sigma-Aldrich) and 0.1% sodium azide with anti-CD16/32 (2.4G2) supernatant (BioXCell), followed by combinations of FITC-, PE-, PerCP-Cy5.5, PE/cyanine 7 (Cy7), PE/Cy5, (allophycocyanin)-, or allophycocyanin/eflour780–conjugated Abs (all from eBioscience); CD62L PE-Texas Red (Invitrogen); CD44-Brilliant Violet 785 (BioLegend, San Diego, CA); and CD5-PE (eBioscience). PSGL-1 PE (BD Biosciences), Ly-6C FITC, CD25 PE-Cy7 (eBioscience), and CXCR5-Biotin, followed by StreptavidineFluor 450. Cells were collected on a LSRII Fortessa using FACSDiva software (BD Biosciences, San Jose, CA) and analyzed in FlowJo (version 9.7) (Tree Star, Ashland, OR). Surface-stained cells were washed with PBS and resuspended in 100 μM Annexin V Ab in proprietary buffer (Invitrogen, Grand Island, NY) for 15 min in the dark at room temperature. Cells were analyzed within 1 h of staining. For Bcl-2, cells were fixed in 2% paraformaldehyde (Sigma-Aldrich) and permeabilized using BD Perm/Wash buffer, and cells were stained with Bcl2-PE (BD Biosciences) for 40 min at 4°C and washed. Compensation was performed in FlowJo using single-stained splenocytes (using CD4 in all colors). For presentation, data from three to four mice are concatenated to achieve sufficient cell numbers for presentation and Boolean gating analysis, after each mouse was analyzed and averages and SEM calculated. For intracellular cytokine and CFSE staining, cells were treated as described previously (17). Gating strategies are shown in Supplemental Fig. 1.

Cell sorting

Splenic $CD4^{+}$ T cells from day 8–infected B5 TCR Tg donors were purified by EasySep biotin selection kit (Stemcell Technologies, Vancouver, BC, Canada) using biotinylated anti-CD8α (55-6.7), B220 (RA3-6B2), CD11b (MI/70), CD11c (N418), F4/80 (BM8), and Ter119 (eBioscience). Enriched T cells were then stained with anti-CD4-FITC, CD44-allophycocyanin-Cy7, CD127-PE, CD62L-Texas Red and CD27-allophycocyanin for Teff subset sorts. Cells were sorted on a FACSAriaI with FACDiva software (BD biosciences). Naive ($CD44^{lo}CD25^{-}$) or effector ($CD44^{int\text{-}hi}CD127^{neg}$) $CD4^{+}$ T cells were sorted from 5- to 12-wk-old B5 TCR Tg mice and transferred i.p. Transfer of 1 million cells models the physiological precursor number of MSP1-specific CD4 T cells seen in the memory phase of infection (0.01% or 1/8800), as previously shown by limiting dilution analysis of splenocytes for responsiveness to this fragment of MSP-1 (33). We have also replicated results in this system with as few as 5000 cells (17). Gating strategy and purity are shown in Supplemental Fig. 1.

Real-time PCR

RNA from purified B5 TCR Tg Teff cell subsets (spun into RLT buffer [Qiagen Valencia, CA] every hour) was analyzed by real-time PCR using a custom PrimePCR assay (Bio-Rad, Hercules, CA) with SYBR green iQ Supermix, and iScript (Bio-Rad) for cDNA synthesis. Normalized relative expression was calculated using GAPDH primers run on each plate as an internal control. Threshold cycle (CT) of the gene of interest (2^[CT of gene of interest − CT GAPDH]) was compared in two subsets ($Teff^{Int}$/$Teff^{Early}$ (Fig. 3B) or relative to naive (Fig. 3C) using Microsoft Excel or Spotfire software for heat map, using the z-score to display relative expression of each gene (TIBCO software).

Statistics

Where indicated, experiments were analyzed by one-way ANOVA, followed by Student *t* test or Tukey's or Wilcoxon rank-sum test for nonparametric data in Prism (GraphPad, La Jolla, CA): $*p \leq 0.05$, $**p \leq 0.01$, $***p \leq 0.001$.

Results

Teff subsets mark progressive activation

Although significant work has been done to understand the differentiation of CD4 Tmem in vivo, the pathway for the development of memory cells from responding Teff remains unclear, especially in chronic infection. In the current study, we sought to demonstrate the cellular pathway of activation of effector CD4 T cells in malaria infection and to use the MSP1-specifc TCR Tg model in BALB/c to identify Teff with the potential to survive through the contraction phase and form protective Tem. To do this, we found it essential to identify subsets of responding Th1 cells that represent progressively activated Teff. To observe the kinetics of *Ifng* expression in responding CD4 T cells in *P. chabaudi* infection and the phenotypes of *Ifng*$^+$ effector cells, we took advantage of an IFN-γ reporter mouse on a polyclonal C57BL/6 background where cells express Thy1.1 transiently on the surface when the *Ifng* gene is transcribed (*Ifng/Thy1.1* knockin). These mice were infected with *P. chabaudi*, and the phenotype of the Teff during expansion was determined on days 5, 7, and 9 p.i. and during the contraction phase as measured on day 12 p.i. Gating on CD127$^-$ Teff, as shown in Supplemental Fig. 1, we observed three Teff subsets (CD62L^{hi}CD27$^+$, CD62L^{lo}CD27$^+$, and CD62L^{lo}CD27$^-$), which appeared to change in proportion over time in response to *P. chabaudi* infection (Fig. 1A). The CD62L^{hi}CD27$^+$ Teff population was enriched on day 5 p.i, and decreased by day 7, whereas the CD62L^{lo}CD27$^+$ and CD62L^{lo}CD27$^-$ Teff were enriched by day 9–12, correlating with the peak of infection (days 8–10) in this model (Fig. 1A, graph). Within *Ifng*/Thy1.1$^+$CD4$^+$ T cells, we observed that an average of 95% of the responding cells were CD127$^-$ on day 9 p.i. (Fig. 1B), indicating that they were indeed activated effector cells (17, 32), and contained all three of the observed subsets. The CD62L^{lo}CD27$^+$ effector population was the highest in IFN-γ production, and numbers of all Teff subpopulations increased to day 9 postinfection and decreased by day 12, as parasite was cleared. The highest levels of T-bet were observed on the CD62L^{lo}CD27$^-$ subset on days 5 and 9 p.i. (Fig. 1C), suggesting full effector activation. As we previously showed a linear path of differentiation for memory cells from CD62L^{hi}CD27$^+$ Tcm to CD62L^{lo}CD27$^+$ early Tem to CD62L^{lo}CD27$^-$ late Tem (17), we hypothesized a similar effector progression from CD62L^{lo}CD27$^+$ to CD62L^{lo}CD27$^-$ Teff before deletion in the contraction phase. We have therefore named these CD4$^+$CD127$^-$ effector populations early (Teff^{Early}; CD62L^{hi}CD27$^+$), intermediate (Teff^{Int} CD62L^{lo}CD27$^+$), and late (Teff^{Late}; CD62L^{lo}CD27$^-$) Teff and tested this progression in this paper.

We sought to test the hypothesis of progressive Teff activation in this C57BL/6 model by using recently reported markers of early Teff/pre-Tcm and late Teff/Th1 cells (26, 27). We therefore validated the overlap of pre-Tcm in effector subsets defined by CD62L and CD27 (Supplemental Fig. 2A) and measured enrichment for pre-Tcm and terminal effectors defined as PSGL-1$^+$Ly6C$^-$ (Supplemental Fig. 2B) and CXCR5$^+$CD25$^-$ (Supplemental Fig. 2C). Interestingly, the pre-Tcm population was enriched in the CD62L^{hi}Teff^{Early} population described in this study, as measured by CXCR5$^+$PSGL1$^+$, and Th1 and T follicular helper (Tfh) terminal effector cells are enriched in CD62L^{lo} late and intermediate Teff (Supplemental Fig. 2D).

Malaria-specific CD4 Teff are progressively activated synchronously

To show that malaria-specific T cells progress through these clearly defined Teff phases, we used a transgenic mouse that expresses a TCR specific for the *P. chabaudi* MSP-1 (B5 Tg). Naive (CD4$^+$CD44^{lo}CD25$^-$) B5 TCR Tg T cells were adoptively transferred (10^6) into congenic Thy1.1 mice, which were subsequently infected with *P. chabaudi.* The cells were recovered on day 9 p.i. and gated on divided cells (CFSE$^-$) to identify responding Teff, which are predominantly CD127$^-$ (Fig. 2A). As seen in the polyclonal system, we observed that within the CD127$^-$ Teff population there are three populations as defined by CD27 and CD62L. We found that CFSE$^-$CD127$^-$CD62L^{hi}CD27$^+$ early effector cells constitute an average of 6.5% of malaria-specific Teff on day 9 p.i. When day 9 B5 TCR Tg cells were gated on CD127$^-$ Teff, we observed that the CD62L^{hi}CD27$^+$ population contained all of the CFSE^{hi} cells (Fig. 2B), suggesting that they are the first to divide. Following the kinetics of development, we observed that on day 5 p.i., B5 Tg Teff were primarily CD27$^+$CD62L^{hi}

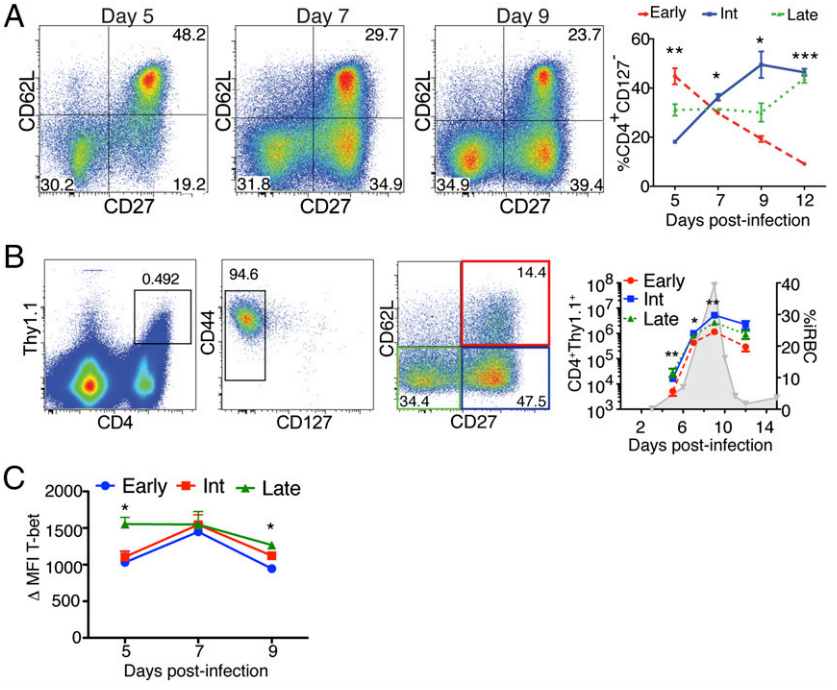

FIGURE 1. IFN-γ$^+$ cells contain three subsets in the effector population. *Ifng/Thy1.1* reporter mice were infected with *P. chabaudi*. (**A**) Proportions of the Teff subsets identified by CD62L and CD27 were determined within CD4$^+$CD127$^-$ on days 5, 7, 9 through 12, and quantification is shown in graph. (**B**) Teff (Thy1.1$^+$CD127$^-$CD44^{hi}) on day 9 p.i. and proportions of effector subsets (right plot) with numbers (graph) of cytokine producers (CD4$^+$*Ifng*/Thy1.1$^+$CD127$^-$) in each Teff subset over the course of infection with parasitemia in shaded gray area. (**C**) Mean fluorescence intensity (MFI) of T bet$^+$ cells in CD4$^+$*Ifng*/Thy1$^+$ cells on days 5, 7, and 9. Data are representative of two experiments with three mice per group. Error bars represent SEM; Student *t* test was used to compare Teff^{Early} versus Teff^{Int} on the same day. $*p < 0.05$, $**p < 0.01$, $***p < 0.001$. Early (Teff^{Early}; CD62L$^+$CD27$^+$), intermediate (Teff^{Int}; CD62L$^-$CD27$^+$), and late (Teff^{Late}; CD62L$^-$CD27$^-$).

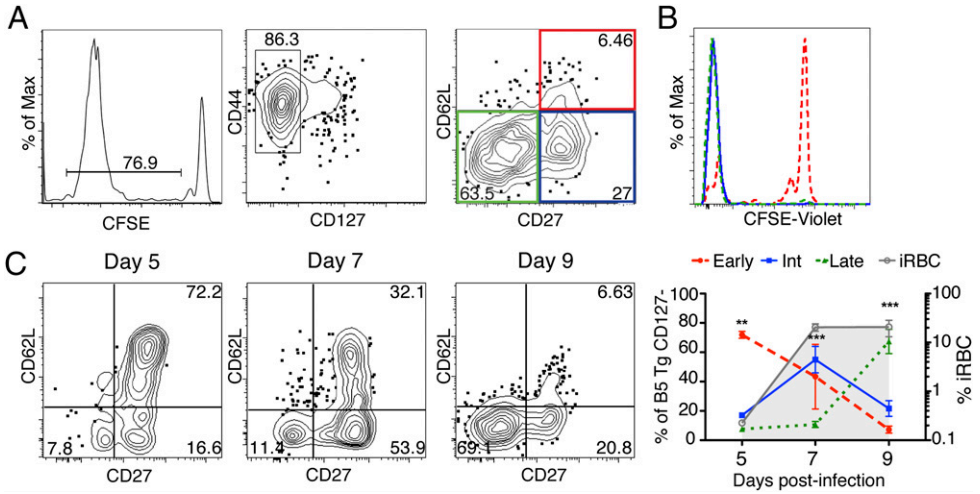

FIGURE 2. The Teff subsets define progressive activation. Naive B5 TCR Tg T cells ($CD44^{lo}CD25^{-}$) were transferred ($1–2 \times 10^6$) into Thy1.1 congenic mice that were subsequently infected with *P. chabaudi*. Splenocytes were analyzed by flow cytometry. (**A**) Dividing, malaria-specific Teff ($CFSE^{-}Thy1.2^{+}CD127^{-}$) day 9 p.i. include early (red; $CD629L^{hi}CD27^{+}$), intermediate (blue; $CD62L^{lo}CD27^{+}$), and late (green; $CD62L^{lo}CD27^{-}$) effector subsets. (**B**) B5 TCR Tg donor cells ($CD4^{+}Thy1.2^{+}CD127^{-}$) showing proliferation of early, intermediates, and late as measured by CFSE-violet dilution at day 9 p.i. (**C**) B5 TCR Tg donor cells ($CD4^{+}Thy1.2^{+}$) showing changing phenotype of Teff ($CD127^{-}$) from days 5 to 9 p.i. Data are concatenated from three recipient hosts and quantified (*right panel*). Parasitemia is shown in shaded gray area. Gates and quadrants are set on all $CD4^{+}$ cells. Error bars represent SEM; *t* test was used to compare the subsets on the same day. $^{**}p < 0.01$, $^{***}p < 0.001$.

early effector cells (average 71.9%; Fig. 2C). The $CD62L^{lo}$ subsets began to increase on day 7, with the $CD27^{+}$ (average 54.95%) preceding the $CD27^{-}$ Teff on day 9 p.i. (average 67.3%), suggesting that the B5 Tg T cells progress through activation in a synchronized manner. The sequential proportional increase of these three Teff subsets during infection further confirmed our hypothesis that they represent a linear progressive activation of T cells in response to malaria infection.

To test this hypothesis at the molecular level, we investigated the expression of pro- and antisurvival factors in these activation subsets. We measured expression of the antiapoptotic molecule Bcl-2 and markers of terminal differentiation (PD-1, Fas, and Annexin V binding) in adoptively transferred B5 TCR Tg cells on day 7 p.i. (Fig. 3A). Only $CD127^{-}CD62L^{hi}$ early B5 Teff cells expressed high levels of Bcl-2, whereas the $CD62L^{lo}$ subsets were Bcl-2^{-} and expressed the inhibitory receptor PD-1 and death domain–containing receptor Fas, suggesting terminal differentiation of the $CD62L^{lo}$ subsets. Supporting this conclusion, $CD27^{-}Teff^{Late}$ had the highest expression of Annexin V^{+}, suggesting that these cells had entered early apoptosis. As an indication of the maturation of functional avidity of the developing Teff, we measured the expression of CD5, an inhibitor of TCR signaling (34). We observed progressive decline in the expression of CD5 from $Teff^{Early}$ to $Teff^{Int}$ and $Teff^{Late}$ cells (Fig. 3A), suggesting that as cells become more activated, they decrease regulation of the TCR and increase in signal strength, thereby correlating with a gain in functional avidity with increasing activation (35). We also measured mRNA levels of other pro- and antiapoptotic molecules by real-time PCR of B5 TCR Tg T cells (Fig. 3B). In the transition from early ($CD62L^{hi}CD27^{+}$) to intermediate ($CD62L^{lo}CD27^{+}$) effectors, we detected significant upregulation of proapoptotic (*fas*, *bcl2l15* [Bfk]), and *bbc3* [Puma], but not *bak1* or *bax*) and downregulation of antiapoptotic (*bcl2*, *mcl1*, *pim2*, and *pim3*) genes at the transcrip-

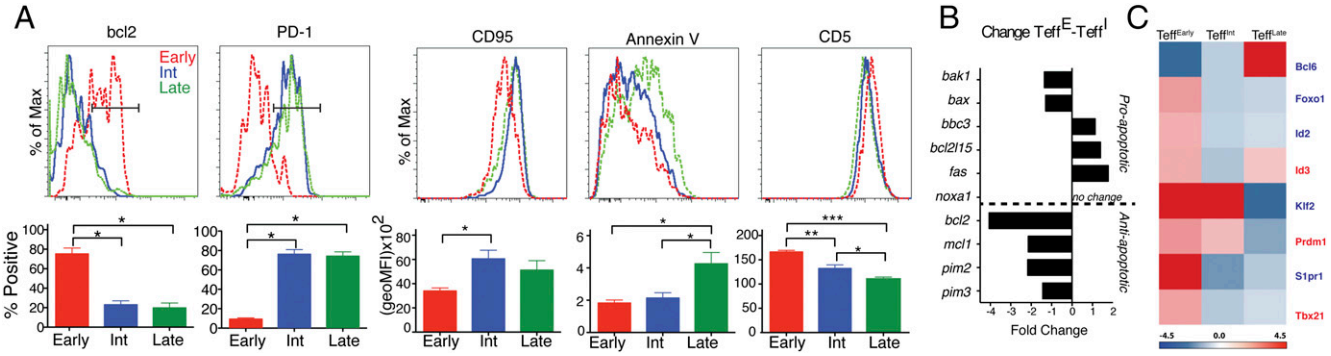

FIGURE 3. Mature Effector T cells are terminally differentiated. Naive B5 TCR Tg CD4 T cells (1×10^6) were transferred into Thy1.1 mice subsequently infected with *P. chabaudi*. Splenocytes were stained for Teff subsets (as defined in Fig. 2) and Bcl-2, PD-1, CD95, Annexin V, and CD5 (**A**) were determined. Plots show representative histograms, whereas graphs (below plots) show percent quantification for Bcl-2 and PD1 on day 7 p.i. or mean fluorescence intensity (MFI) for CD95, Annexin V, and CD5 on day 16 p.i. of positive cells in the histograms for all the subsets. Data are concatenated for B5 TCR Tg cells from three mice and are representative of two independent experiments. Gates set on isotype controls, but isotype and positive controls are not shown for clarity. Error bars represent SEM comparing different subsets on the same day. (**B**) Expression of selected pro- and antiapoptotic genes showing fold change from early to intermediate on day 8 p.i. of sorted Teff subsets. (**C**) Effector (labeled in red) and memory (labeled in blue) gene expression for the three Teff subsets. PCR data were normalized to GAPDH and z-score of relative expression of each gene compared with naive across the subsets is shown. Error bars represent SEM; *t* test was used to compare the subsets. $^{*}p < 0.05$, $^{**}p < 0.01$, $^{***}p < 0.001$.

tional level (Fig. 3B). Because the Teff^{Early} express high levels of prosurvival molecules suggesting longevity, we also measured expression of memory and effector differentiation genes (Fig. 3C). Interestingly, Teff^{Early} expressed higher levels of memory genes including (*foxo1*, *id2*, *klf2*, and *S1pr1*) as well as Teff genes (*id3*, *prdm1*, and *tbx21*) than the other two subsets. A notable exception is *Bcl6*, which is reported to be a memory promoting transcription factor (36), but is not increased in early CD4 effector cells in this infection. Taken together, these data suggest that early-activated CD4 Teff contain a longer-lived pre-Tmem population, whereas the highly activated CD62L^{lo} cells appear terminally differentiated. To study the progression of effector cytokine production during activation, we determined the cytokine profile of the malaria-specific Teff subsets by intracellular cytokine staining in adoptively transferred B5 TCR Tg cells on day 7 p.i. The CD62L^{lo}CD27^{-} Teff^{Int} subset contained the highest percentage of cytokine producers for IFN-γ, TNF-α, and IL-2 (Fig. 4A), showing that this is the most responsive subset. Interestingly, some Teff^{Early} also make cytokines; however, 40% of Teff^{Early} cytokine producers are TNF^{+}IL-2^{+}, which is the cytokine profile of CD4 Tcm (17, 37, 38). Furthermore, only the CD62L^{lo} Teff subsets (Teff^{Int} and Teff^{Late}) contain triple cytokine producers (TNF^{+}IFN-γ^{+}IL-2^{+}; Fig. 4B), indicating that the multicytokine-producing phenotype is associated with highly activated effectors at this stage of infection.

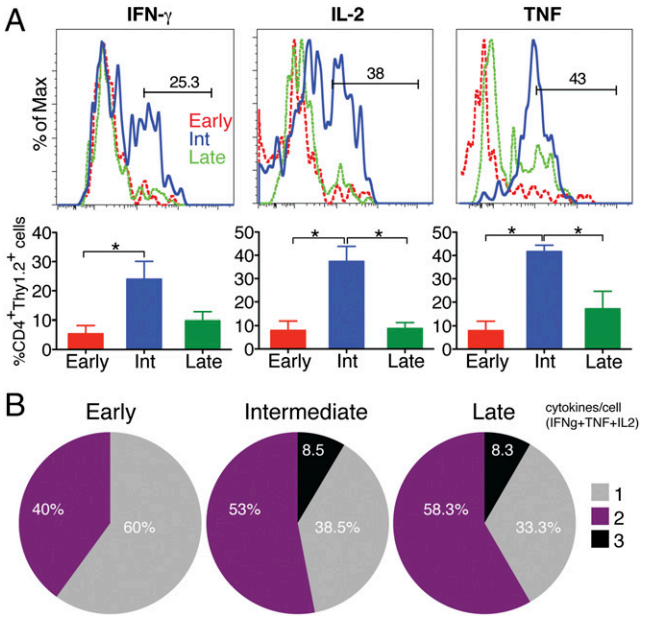

FIGURE 4. Mature Effector T cells are multicytokine producers. Naive B5 TCR Tg CD4 T cells (1×10^6) were transferred into Thy1.1 mice subsequently infected with *P. chabaudi*. Splenocytes were stained day 7 p.i. for Teff subsets (as defined in Fig. 2), and cytokine secretion of the subsets was determined using intracellular staining. (**A**) Histograms of cytokine profile of each Teff (CD4^{+}CD127^{-}) subset day 7 p.i. after adoptive transfer, including early (red; CD62L^{hi}CD27^{+}), intermediate (blue; CD62L^{lo}CD27^{+}), and late (green; CD62L^{lo}CD27^{-}) effector cells are shown. Isotype controls were used to define positive gates (data not shown for clarity). The plots represent percent quantification of all the mice in the experiment. (**B**) Pie charts show percentage of B5 Tg cytokine–producing cells in each subset expressing one to three cytokines as calculated by Boolean analysis. Data represent concatenated B5 TCR Tg cells from three mice and are representative of two independent experiments. Error bars represent SEM, comparing different groups. *$p < 0.05$.

CD62L^{lo} classical Teff subsets are short-lived effector cells

On the basis of the expression of memory and antiapoptotic genes and the timing of their appearance, we hypothesized that early effector cells may survive the contraction phase and contribute to memory differentiation, whereas CD62L^{lo} subsets would lose this potential. Therefore, we determined the fate of each effector subset over the peak of infection and observed survival in the contraction phase. Teff subsets were sort purified from infected B5 TCR Tg mice (day 8 p.i.), based on the gating strategy and purity shown in Supplemental Fig. 1C–E. Each subset was transferred into infection-matched Thy1.1^{+} congenic recipients days 8 through 11 of infection (Fig. 5). Despite historic reluctance to infect intact TCR-transgenic animals in favor of adoptive transfer, we have previously verified similar degrees of T cell activation in B5 TCR Tg and wild-type animals and found phenotypes and protection comparable (17). Adoptive transfer of the three purified Teff populations at the peak of infection into infection-matched recipients showed that only the Teff^{Early} population was capable of surviving 3 d of infection during the contraction phase (Fig. 5A), demonstrating that early CD62L^{hi} effector cells could survive the T cell contraction during parasite clearance. The CD62L^{lo} Teff were terminally differentiated because there were minimal T cell numbers recovered from the recipients of these subsets. Furthermore, the recovered Teff^{Early} cells generated both Teff^{Int} and Teff^{Late} populations after 3 d (Teff^{Early} OUT) in this period of the T cell response when the parasitemia is decreasing and the T cells are contracting (as seen in Fig. 1B).

To test the survival potential of the three subsets of effector cells in the absence of Ag, we investigated their phenotype on recovery from an uninfected recipient. We transferred each purified Teff subset into uninfected congenic Thy1.1 hosts and analyzed the recovery and phenotype of the cells 14 d after transfer. Again, we recovered significantly higher numbers of B5 TCR Tg T cells from recipients of Teff^{Early} than Teff^{Int} or Teff^{Late} (Fig. 5B). Interestingly, in the absence of Ag, an average of 65% of the recovered CD127^{-} Teff retained their original CD62L^{hi}CD27^{+} phenotype and did not progress as in the infection-matched recipients (Fig. 5B, Teff^{Early} OUT, Teff pie chart), indicating that infection promotes the progressive activation through these phenotypes from CD62L^{hi} to CD62L^{lo}CD27^{-} (Fig. 5). Furthermore, on transfer, they had been completely CD127^{-}, whereas after 2 wk without parasite exposure, the majority reupregulated CD127 to become CD127 intermediate (average 61.5%). To identify true memory phenotype cells, we gated on the CD127^{hi} and identified both Tcm and Tem derived from the Teff^{Early} (Fig. 5B, Teff^{Early} OUT, Tmem pie chart). These data suggest that the Early Teff subset can make all the later Teff subsets in the presence of Ag and a fraction can also survive the contraction and potentially make Tmem upon Ag elimination.

Ag and IL-2 are important in progressive activation of Teff

Because Teff expand in response to IL-2, we predicted that blocking IL-2 would impede progressive differentiation of the Teff subsets. We therefore administered anti–IL-2 over the first 9 d of infection to Thy1.1 congenic recipients of B5 TCR Tg CD4 T cells (Fig. 6). Unexpectedly, there was a significant decrease in the proportion of the Teff^{Early}, as opposed to an increase, and an increase in the terminal MSP-1–specific Teff subsets in the anti–IL-2–treated animals compared with isotype controls on day 5 p.i., which persisted through day 9 (Fig. 6A–C), although the differences seen on day 9 were not statistically significant. As expected, animals treated with anti–IL-2 did not have significant T cell accumulation by day 9 p.i. (Fig. 6D), when T cell numbers are

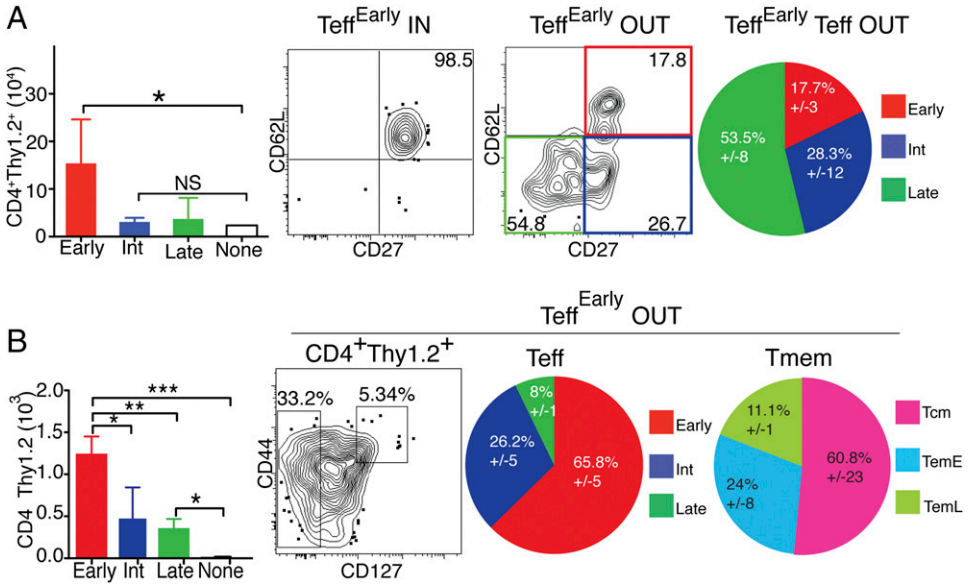

FIGURE 5. Teff^{Early} subset generates all effector and memory subsets. Malaria-specific B5 CD4$^+$ Teff subsets were sorted on day 8 p.i. and transferred (7×10^5) into infection-matched (**A**) or naive Thy1.1 recipients (**B**). (A) Numbers (*left panel*) and phenotype of sorted (IN) and of recovered (OUT) donor cells (CD4$^+$Thy1.2$^+$) were determined on day 3 posttransfer (day 11 p.i.) in infection-matched recipients. Purity of sorted Teff^{Early} (IN) and CD4$^+$Thy1.2$^+$CD127$^-$ cells recovered from Teff^{Early} recipients (OUT) is shown. (B) Numbers (*left panel*) and phenotype of recovered (OUT) early donor cells (CD4$^+$Thy1.2$^+$) were determined on day 14 posttransfer in naive recipients. All recovered cells are represented as contour plots with outliers. Pie charts show percentage of each Teff (CD127$^-$) subset (*left pie chart*) or Tmem (CD127^{hi}) subset (*right pie chart*) within recovered early subset. Error bars represent SEM; data were analyzed by one-way ANOVA, followed by Tukey's test comparing all the groups. $^*p < 0.05$, $^{**}p < 0.01$, $^{***}p < 0.001$.

at their peak in this infection. These data suggest that progressive differentiation of the Teff from early to late activation is slowed by IL-2 and that licensing of full effector activation and T cell expansion are separable.

Because the duration and strength of Ag stimulation has been proposed to determine the extent of CD4 T cell activation and differentiation (29), and this has been persuasively shown for CD8 T cells (39), we tested whether shortening the period of infection would affect the full activation of Teff and the ratio of memory subsets generated. Adoptively transferred recipient mice were infected but treated with MQ, an antimalarial drug, on days 3–5 (MQ d3) or 5–7 (MQ d5) p.i. to reduce the load of parasitemia, or left untreated, and Teff phenotype was determined in all the mice on day 9 p.i. (Fig. 7A). There were strikingly higher proportions of the CD127$^-$CD62L^{hi}CD27$^+$ Teff^{Early} subset on day 9, when parasite grew unimpeded for only 3 d, with intermediate levels of Teff^{Early} population in MQ d5 treated animals. This decreased to 4.4% Teff^{Early} (average) when mice were not treated, suggesting that a longer duration of parasitemia indeed induced a stronger total signal and pushed the effector cells through the phases of Teff activation from Teff^{Early} to Teff^{Late}. Early Ag elimination was also accompanied by a significant increase in CD44^{hi}CD127^{hi} cells (data not shown), indicating the possibility of early memory generation.

Our previous work shortening the infection with chloroquine on day 30, did not change the Tcm to Tem ratio (17). To determine whether earlier elimination of Ag might influence the transition of Teff into memory, we treated the recipient mice with MQ on days 3–7 and analyzed memory cell formation on day 53 p.i. As a control, we treated another group with chloroquine days 30–34 to eliminate parasite exposure for the three weeks before analysis for Tmem. We observed a significantly higher proportion of CD127^{hi}CD62L^{hi}CD27$^+$ Tcm in the mice treated with MQ on day

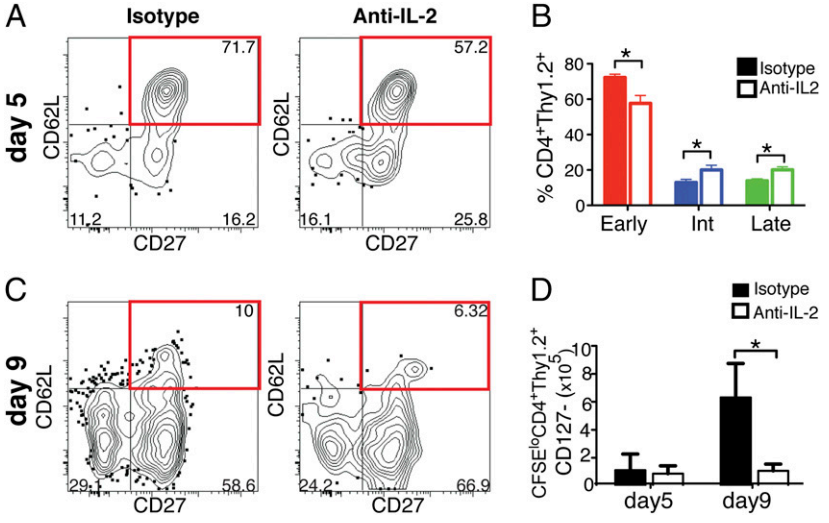

FIGURE 6. IL-2 deprivation promotes Teff progression. Naive B5 TCR Tg CD4 T cells (1×10^6) were transferred into Thy1.1 mice subsequently infected with *P. chabaudi*. Mice were treated with anti–IL-2 on alternate days starting day 1 p.i. Splenocytes were stained for B5 Teff subsets as in Fig. 3. (**A**) Plots of Teff subsets comparing isotype to anti–IL-2 treatment on days 5 p.i. (**B**) The percentage of each Teff subset out of CFSE^{lo}Thy1.2$^+$CD127$^-$ Teff on day 5 p.i. (**C**) Plots of Teff subsets on day 9 comparing isotype to anti–IL-2. (**D**) Absolute cell numbers of proliferating effector (CFSE^{lo}CD127$^-$) B5 subsets on days 5 and 9 p.i. The plots are representative of one mouse from a group of four to five mice. Data were analyzed using Student *t* test and shows mean and SEM. $^*p < 0.05$.

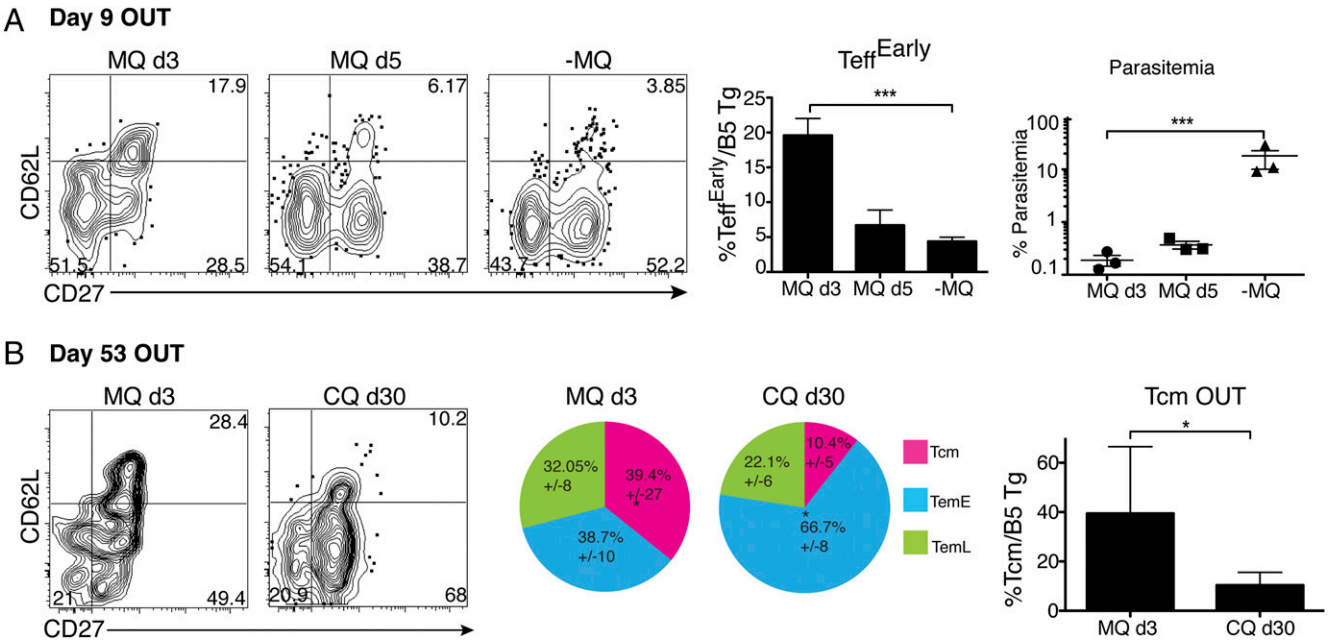

FIGURE 7. Ag drives the progressive activation of the Teff subsets. Naive B5 TCR Tg CD4 T cells (1×10^6) were transferred into Thy1.1 mice subsequently infected with *P. chabaudi*. (**A**) Mice were treated with MQ on days 3–5 or 5–7 and Teff subset phenotypes were determined on day 9 p.i. Plots show phenotype of $CD4^+CFSE^-CD127^-$ T cell subsets from day 3, day 5m and no treatment groups. Data represent one mouse of three mice per group. Graphs show quantification of the $CD127^-CD62L^{hi}CD27^+$ $Teff^{Early}$ subset or parasitemia in the three groups. Student *t* test was used to compare the MQ treated versus not treated (NT), and error bars represent SEM. (**B**) Mice were treated with MQ (days 3–7) or CQ (days 30–34), and phenotypes of memory subsets were determined on day 53 p.i. Plots show phenotypes of memory subsets ($CD4^+CD127^+$), whereas pie charts show quantification of Tmem in the two groups. The numbers in the pies represent average and SEM of all mice in each group. The graph shows total numbers of recovered cells. Student *t* test was used to compare MQ- versus CQ-treated groups, and error bars represent SEM. $*p < 0.05$, $***p < 0.001$.

3 compared with those exposed to a full infection (Fig. 7B), and a correspondingly higher proportion of $CD127^{hi}CD62L^{hi}CD27^+$ early Tem in mice exposed to infection for a month, suggesting that exposure to chronic infection induces Tem, while shorter exposure to the same parasite induces Tcm. Unsurprisingly, there were also significantly more total cells recovered from the animals with the full month of infection. Although this agrees with previous studies suggesting that chronicity generates Tem, it is striking how early the infection had to be treated to reduce Tem generation.

Discussion

In the current study, we have identified a pathway of progressive activation of effector CD4 T cells in malaria infection to generate Tmem. We have described three subsets of effector cells, identified by their transient downregulation of CD127, that define the gamut of activation states leading to terminal differentiation versus memory survival. The earliest of these activation states is a population quickly re-expressing CD62L (31), which potentially contains both short-lived effector cells and memory precursor effector cells. We show that effector cells go through a linear pathway of activation starting from an early $CD127^-CD62L^{hi}$ Teff precursor, which are the least divided, and are not terminally differentiated likely because of higher expression of prosurvival genes. The later, $CD62L^{lo}$, stages include $CD27^-$ late effector cells that express PD-1, Fas, and Annexin V^+, indicating early stages of cell death, and $CD27^+$ $Teff^{Int}$, with the maximum effector function. We show that highly activated CD4 Teff lose the ability to survive after the contraction phase, whereas the $CD62L^{hi}$ $Teff^{Early}$ are recovered both after contraction and after being "rested" in naive hosts and have the phenotypes of both Tcm and Tem.

To our knowledge, this work is the first step to defining the fate of various CD4 effector cells generated in parasitic infections and may eventually contribute to resolving the controversial derivation of Tem because they can derive from both IFN-γ–producing (25, 40, 41) and IFN-γ^- Teff (42). Residual Teff have also been identified several months postinfection (14, 17, 27, 43–45), suggesting that some cells with Teff phenotypes survive beyond contraction. In contrast, it has also been suggested in the progressive differentiation model for CD4 T cell differentiation that Tem are generated from fully activated effector cells (25, 27), although this is hard to reconcile with the abovementioned data. The progressive activation states and terminal differentiation of Teff demonstrated in this study support the current paradigm from studies in CD8 T cells that, as Teff become progressively activated, they lose the potential to generate Tmem (39). Our data suggest that like effector CD8 T cells ($KLRG1^+$, $Ly6C^{hi}$), CD4 T cells lose their potential to generate memory with increasing activation, and in the case of CD8 cells, with exposure to IL-12 and increased T-bet expression (46, 47), suggesting that highly activated T cells are terminal and not likely to survive past the contraction. Supporting this interpretation, Tem and Tmem differentiation appear to be mutually exclusive because they are regulated by pairs of transcription factors including T-bet and eomes, Id3 and Id2, and Blimp and Bcl6, which each promote terminal differentiation over Tmem development, respectively (39, 48, 49).

Several studies indicate that memory cell precursors can be detected during the early stages of activation in other models and infections (26, 50). In this study, we used CD127 downregulation to mark Teff because effector cells from the peak of infection are $CD127^-$ (17). Our $CD62L^{hi}Teff^{Early}$ effector population overlaps significantly with early effector $CXCR5^+CD25^-$ cells proposed to

be pre-Tcm by Pepper et al. (26, 27), whereas the CD62L^{lo} populations contain terminal effector cells. We show that the low proportional enrichment of Ly6C^{+} in later populations is due to a large expansion of the CXCR5^{+} population, which has been shown to contain a mixture of Tfh and pre-Tcm (51). In *P. chabaudi* infection, we see a large expansion of CXCR5^{+} effector cells that are Tbet^{+} (V.H. Carpio, M.M. Opata, and R. Stephens, manuscript in preparation), and in this study, we show that CD62L^{lo} Teff^{Int} and Teff^{Late} CXCR5^{+} cells are also PSGL-1^{lo} Ly6C^{-}, suggesting that the CD62L^{lo} Teff contain Th1 and Tfh effector cells but not pre-Tcm, thereby correlating all three definitions of the late subsets. Therefore, our work suggests that CD62L^{hi}CXCR5^{+} are pre-Tcm, whereas CD62L^{lo}CXCR5^{+} may be Tfh effector cells.

Because Teff^{Early} can generate both Teff^{Late} and memory cells, it is likely that the Teff^{Early} subset described in this paper contains the precursors of both effector and memory cells, as also suggested by the representation of Ly6C^{+} population in the Teff^{Early}. Consistent with this, we observe an enrichment of both effector-associated and memory-associated genes in Teff^{Early} compared with the Teff^{Int} and Teff^{Late} effector subsets. This is consistent with a very early decision point, such as that provided by asymmetrical division (52). Nevertheless, CD62L^{hi}Teff^{Early} is clearly the Teff subset containing the long-lived precursors of CD4 Tmem.

By precisely measuring degrees of Teff activation in a linear pathway and neutralizing IL-2, we show that the T cell growth factor, IL-2, while essential for CD4 T cell proliferation, also has a role in regulating the pace of progression through these activation states. Without IL-2, progression through the spectrum of activation is increased, suggesting a more rapid development of a highly activated but terminally differentiated late Teff phenotype in the absence of this important proliferation-inducing factor. This is consistent with previous studies showing that IL-2 plays a role during the T cell expansion phase in generation of functional CD4 memory cells (53, 54).

The role of Ag in the generation and maintenance of protective Tmem is an active area of research. We had previously shown that treatment of *P. chabaudi* infection on day 30 had no effect on the ratios of Tcm to Tem (17); however, by treating the infection and exposing the T cells to either 3 or 30 d of malaria infection, we have shown that only a very short exposure to the infection increases the durable Teff^{Early} population. Interestingly, elimination of parasite on day 3 led to a higher proportion of Tcm at day 53 p.i., whereas day 30–treated mice had more Tem, and higher cell numbers supporting the hypothesis that chronic infection drives Tem generation and providing the additional insight that the change from Tcm generation to Tem generation depends on very quick control of infection. Similarly, some studies on development of CD8 memory have shown that the cumulative degree of activation, determined by the type and duration of stimuli early in activation, can determine effector versus memory fate of the responding cells (55–57). Additional signals such as production of survival cytokines, even later in infection, are also likely to affect the subset ratios over time (58). If prolonged Ag or cytokine exposure leads to a loss in these long-lived cells, this could be one reason why people in malaria endemic areas do not quickly develop immunity to infection.

Although there is no good protection from malaria infection, there is protection from severe disease, which may be T cell mediated. We have shown that early effector T cells in this model infection can in fact survive to the memory stage and make both Tcm and Tem phenotype cells, which are likely to balance the pathology of reinfection. Further elucidation of their ability to protect and maintain this protection are an important focus of future studies. Because Tem is the predominant memory subset generated by chronic infections like malaria and tuberculosis (16, 17, 59) and autoimmune diseases (60) and that their differentiation is not currently understood separately from that of effector cells, understanding the development of these potentially longer-lived cells is likely to be critical for the development of successful adjuvants, treatments, and vaccines for chronic T cell–mediated disease.

Acknowledgments

We thank M. C. Griffin for assistance with cell sorting and M. L. Ramirez for animal husbandry. We thank A.L. Miller and R.B. Pyles for the help with the PCR analysis. We also thank Drs. M. Roederer, J.J. Endsley, N.C. Peters, N. Sandler Utay, G. M. Kaus, K.D. Wilson, K.M. Norwood, and M. Susman for thoughtful review of the manuscript.

Disclosures

The authors have no financial conflicts of interest.

References

1. World Health Organization Global Malaria Programme. 2014. *World Malaria Report.* M. Aregawi, R. Cibulskis, C. Fergus, M. Lynch, E. Patoullard, Z. Szilagy, and R. Wlliams, eds, p. 1–242.
2. Langhorne, J., F. M. Ndungu, A. M. Sponaas, and K. Marsh. 2008. Immunity to malaria: more questions than answers. *Nat. Immunol.* 9: 725–732.
3. Marsh, K., and S. Kinyanjui. 2006. Immune effector mechanisms in malaria. *Parasite Immunol.* 28: 51–60.
4. Gupta, S., R. W. Snow, C. A. Donnelly, K. Marsh, and C. Newbold. 1999. Immunity to non-cerebral severe malaria is acquired after one or two infections. *Nat. Med.* 5: 340–343.
5. Meding, S. J., and J. Langhorne. 1991. CD4^{+} T cells and B cells are necessary for the transfer of protective immunity to *Plasmodium chabaudi chabaudi. Eur. J. Immunol.* 21: 1433–1438.
6. Marsh, K., L. Otoo, R. J. Hayes, D. C. Carson, and B. M. Greenwood. 1989. Antibodies to blood stage antigens of *Plasmodium falciparum* in rural Gambians and their relation to protection against infection. *Trans. R. Soc. Trop. Med. Hyg.* 83: 293–303.
7. Su, Z., and M. M. Stevenson. 2000. Central role of endogenous gamma interferon in protective immunity against blood-stage *Plasmodium chabaudi AS* infection. *Infect. Immun.* 68: 4399–4406.
8. Freitas do Rosário, A. P., T. Lamb, P. Spence, R. Stephens, A. Lang, A. Roers, W. Muller, A. O'Garra, and J. Langhorne. 2012. IL-27 promotes IL-10 production by effector Th1 CD4^{+} T cells: a critical mechanism for protection from severe immunopathology during malaria infection. *J. Immunol.* 188: 1178–1190.
9. Portugal, S., J. Moebius, J. Skinner, S. Doumbo, D. Doumtabe, Y. Kone, S. Dia, K. Kanakabandi, D. E. Sturdevant, K. Virtaneva, et al. 2014. Exposure-dependent control of malaria-induced inflammation in children. *PLoS Pathog.* 10: e1004079.
10. Stephens, R., F. R. Albano, S. Quin, B. J. Pascal, V. Harrison, B. Stockinger, D. Kioussis, H.-U. Weltzien, and J. Langhorne. 2005. Malaria-specific transgenic CD4^{+} T cells protect immunodeficient mice from lethal infection and demonstrate requirement for a protective threshold of antibody production for parasite clearance. *Blood* 106: 1676–1684.
11. Stephens, R., R. L. Culleton, and T. J. Lamb. 2012. The contribution of *Plasmodium chabaudi* to our understanding of malaria. *Trends Parasitol.* 28: 73–82.
12. Uzonna, J. E., G. Wei, D. Yurkowski, and P. Bretscher. 2001. Immune elimination of *Leishmania major* in mice: implications for immune memory, vaccination, and reactivation disease. *J. Immunol.* 167: 6967–6974.
13. Bustamante, J. M., L. M. Bixby, and R. L. Tarleton. 2008. Drug-induced cure drives conversion to a stable and protective CD8^{+} T central memory response in chronic Chagas disease. *Nat. Med.* 14: 542–550.
14. Peters, N. C., A. J. Pagán, P. G. Lawyer, T. W. Hand, E. Henrique Roma, L. W. Stamper, A. Romano, and D. L. Sacks. 2014. Chronic parasitic infection maintains high frequencies of short-lived Ly6C^{+}CD4^{+} effector T cells that are required for protection against re-infection. *PLoS Pathog.* 10: e1004538.
15. Achtman, A. H., R. Stephens, E. T. Cadman, V. Harrison, and J. Langhorne. 2007. Malaria-specific antibody responses and parasite persistence after infection of mice with *Plasmodium chabaudi chabaudi. Parasite Immunol.* 29: 435–444.
16. Chelimo, K., P. B. Embury, P. O. Sumba, J. Vulule, A. V. Ofulla, C. Long, J. W. Kazura, and A. M. Moormann. 2011. Age-related differences in naturally acquired T cell memory to *Plasmodium falciparum* merozoite surface protein 1. *PLoS One* 6: e24852.
17. Stephens, R., and J. Langhorne. 2010. Effector memory Th1 CD4 T cells are maintained in a mouse model of chronic malaria. *PLoS Pathog.* 6: e1001208.
18. Zarling, S., D. Berenzon, S. Dalai, D. Liepinsh, N. Steers, and U. Krzych. 2013. The survival of memory CD8 T cells that is mediated by IL-15 correlates with sustained protection against malaria. *J. Immunol.* 190: 5128–5141.

19. Tse, S. W., A. J. Radtke, D. A. Espinosa, I. A. Cockburn, and F. Zavala. 2014. The chemokine receptor CXCR6 is required for the maintenance of liver memory CD8$^+$ T cells specific for infectious pathogens. *J. Infect. Dis.* 210: 1508–1516.
20. Butler, N. S., J. Moebius, L. L. Pewe, B. Traore, O. K. Doumbo, L. T. Tygrett, T. J. Waldschmidt, P. D. Crompton, and J. T. Harty. 2012. Therapeutic blockade of PD-L1 and LAG-3 rapidly clears established blood-stage *Plasmodium* infection. *Nat. Immunol.* 13: 188–195.
21. Illingworth, J., N. S. Butler, S. Roetynck, J. Mwacharo, S. K. Pierce, P. Bejon, P. D. Crompton, K. Marsh, and F. M. Ndungu. 2013. Chronic exposure to *Plasmodium falciparum* is associated with phenotypic evidence of B and T cell exhaustion. *J. Immunol.* 190: 1038–1047.
22. Stephens, R., B. Seddon, and J. Langhorne. 2011. Homeostatic proliferation and IL-7Rα expression do not correlate with enhanced T cell proliferation and protection in chronic mouse malaria. *PLoS One* 6: e26686.
23. Stephens, R., F. M. Ndungu, and J. Langhorne. 2009. Germinal centre and marginal zone B cells expand quickly in a second *Plasmodium chabaudi* malaria infection producing mature plasma cells. *Parasite Immunol.* 31: 20–31.
24. Masopust, D., and L. J. Picker. 2012. Hidden memories: frontline memory T cells and early pathogen interception. *J. Immunol.* 188: 5811–5817.
25. Harrington, L. E., K. M. Janowski, J. R. Oliver, A. J. Zajac, and C. T. Weaver. 2008. Memory CD4 T cells emerge from effector T-cell progenitors. *Nature* 452: 356–360.
26. Pepper, M., A. J. Pagán, B. Z. Igyártó, J. J. Taylor, and M. K. Jenkins. 2011. Opposing signals from the Bcl6 transcription factor and the interleukin-2 receptor generate T helper 1 central and effector memory cells. *Immunity* 35: 583–595.
27. Marshall, H. D., A. Chandele, Y. W. Jung, H. Meng, A. C. Poholek, I. A. Parish, R. Rutishauser, W. Cui, S. H. Kleinstein, J. Craft, and S. M. Kaech. 2011. Differential expression of Ly6C and T-bet distinguish effector and memory Th1 CD4$^+$ cell properties during viral infection. *Immunity* 35: 633–646.
28. Opata, M. M., and R. Stephens. 2013. Early decision: effector and effector memory T cell differentiation in chronic infection. *Curr. Immunol. Rev.* 9: 190–206.
29. Swain, S. L., J. N. Agrewala, D. M. Brown, D. M. Jelley-Gibbs, S. Golech, G. Huston, S. C. Jones, C. Kamperschroer, W. H. Lee, K. K. McKinstry, et al. 2006. CD4$^+$ T-cell memory: generation and multi-faceted roles for CD4$^+$ T cells in protective immunity to influenza. *Immunol. Rev.* 211: 8–22.
30. Mahnke, Y. D., T. M. Brodie, F. Sallusto, M. Roederer, and E. Lugli. 2013. The who's who of T-cell differentiation: human memory T-cell subsets. *Eur. J. Immunol.* 43: 2797–2809.
31. Chao, C. C., R. Jensen, and M. O. Dailey. 1997. Mechanisms of L-selectin regulation by activated T cells. *J. Immunol.* 159: 1686–1694.
32. Huster, K. M., V. Busch, M. Schiemann, K. Linkemann, K. M. Kerksiek, H. Wagner, and D. H. Busch. 2004. Selective expression of IL-7 receptor on memory T cells identifies early CD40L-dependent generation of distinct CD8$^+$ memory T cell subsets. *Proc. Natl. Acad. Sci. USA* 101: 5610–5615.
33. Quin, S. J., E. M. Seixas, C. A. Cross, M. Berg, V. Lindo, B. Stockinger, and J. Langhorne. 2001. Low CD4$^+$ T cell responses to the C-terminal region of the malaria merozoite surface protein-1 may be attributed to processing within distinct MHC class II pathways. *Eur. J. Immunol.* 31: 72–81.
34. Tarakhovsky, A., S. B. Kanner, J. Hombach, J. A. Ledbetter, W. Müller, N. Killeen, and K. Rajewsky. 1995. A role for CD5 in TCR-mediated signal transduction and thymocyte selection. *Science* 269: 535–537.
35. Slifka, M. K., and J. L. Whitton. 2001. Functional avidity maturation of CD8$^+$ T cells without selection of higher affinity TCR. *Nat. Immunol.* 2: 711–717.
36. Ichii, H., A. Sakamoto, M. Arima, M. Hatano, Y. Kuroda, and T. Tokuhisa. 2007. Bcl6 is essential for the generation of long-term memory CD4$^+$ T cells. *Int. Immunol.* 19: 427–433.
37. Reinhardt, R. L., A. Khoruts, R. Merica, T. Zell, and M. K. Jenkins. 2001. Visualizing the generation of memory CD4 T cells in the whole body. *Nature* 410: 101–105.
38. Sallusto, F., D. Lenig, R. Förster, M. Lipp, and A. Lanzavecchia. 1999. Two subsets of memory T lymphocytes with distinct homing potentials and effector functions. *Nature* 401: 708–712.
39. Kaech, S. M., and W. Cui. 2012. Transcriptional control of effector and memory CD8$^+$ T cell differentiation. *Nat. Rev. Immunol.* 12: 749–761.
40. Bannard, O., M. Kraman, and D. T. Fearon. 2009. Secondary replicative function of CD8$^+$ T cells that had developed an effector phenotype. *Science* 323: 505–509.
41. Swain, S. L. 1994. Generation and in vivo persistence of polarized Th1 and Th2 memory cells. *Immunity* 1: 543–552.
42. Wu, C. Y., J. R. Kirman, M. J. Rotte, D. F. Davey, S. P. Perfetto, E. G. Rhee, B. L. Freidag, B. J. Hill, D. C. Douek, and R. A. Seder. 2002. Distinct lineages of T(H)1 cells have differential capacities for memory cell generation in vivo. *Nat. Immunol.* 3: 852–858.
43. Hikono, H., J. E. Kohlmeier, S. Takamura, S. T. Wittmer, A. D. Roberts, and D. L. Woodland. 2007. Activation phenotype, rather than central- or effector-memory phenotype, predicts the recall efficacy of memory CD8$^+$ T cells. *J. Exp. Med.* 204: 1625–1636.
44. Olson, J. A., C. McDonald-Hyman, S. C. Jameson, and S. E. Hamilton. 2013. Effector-like CD8$^+$ T cells in the memory population mediate potent protective immunity. *Immunity* 38: 1250–1260.
45. Ahmadzadeh, M., S. F. Hussain, and D. L. Farber. 2001. Heterogeneity of the memory CD4 T cell response: persisting effectors and resting memory T cells. *J. Immunol.* 166: 926–935.
46. Wilson, D. C., S. Matthews, and G. S. Yap. 2008. IL-12 signaling drives CD8$^+$ T cell IFN-γ production and differentiation of KLRG1$^+$ effector subpopulations during *Toxoplasma gondii* infection. *J. Immunol.* 180: 5935–5945.
47. Intlekofer, A. M., N. Takemoto, E. J. Wherry, S. A. Longworth, J. T. Northrup, V. R. Palanivel, A. C. Mullen, C. R. Gasink, S. M. Kaech, J. D. Miller, et al. 2005. Effector and memory CD8$^+$ T cell fate coupled by T-bet and eomesodermin. *Nat. Immunol.* 6: 1236–1244.
48. Crotty, S., R. J. Johnston, and S. P. Schoenberger. 2010. Effectors and memories: Bcl-6 and Blimp-1 in T and B lymphocyte differentiation. *Nat. Immunol.* 11: 114–120.
49. Yang, C. Y., J. A. Best, J. Knell, E. Yang, A. D. Sheridan, A. K. Jesionek, H. S. Li, R. R. Rivera, K. C. Lind, L. M. D'Cruz, et al. 2011. The transcriptional regulators Id2 and Id3 control the formation of distinct memory CD8$^+$ T cell subsets. *Nat. Immunol.* 12: 1221–1229.
50. Obar, J. J., and L. Lefrançois. 2010. Early signals during CD8 T cell priming regulate the generation of central memory cells. *J. Immunol.* 185: 263–272.
51. Choi, Y. S., J. A. Yang, I. Yusuf, R. J. Johnston, J. Greenbaum, B. Peters, and S. Crotty. 2013. Bcl6 expressing follicular helper CD4 T cells are fate committed early and have the capacity to form memory. *J. Immunol.* 190: 4014–4026.
52. Chang, J. T., M. L. Ciocca, I. Kinjyo, V. R. Palanivel, C. E. McClurkin, C. S. Dejong, E. C. Mooney, J. S. Kim, N. C. Steinel, J. Oliaro, et al. 2011. Asymmetric proteasome segregation as a mechanism for unequal partitioning of the transcription factor T-bet during T lymphocyte division. *Immunity* 34: 492–504.
53. McKinstry, K. K., T. M. Strutt, B. Bautista, W. Zhang, Y. Kuang, A. M. Cooper, and S. L. Swain. 2014. Effector CD4 T-cell transition to memory requires late cognate interactions that induce autocrine IL-2. *Nat. Commun.* 5: 5377.
54. MacLeod, M. K., A. McKee, F. Crawford, J. White, J. Kappler, and P. Marrack. 2008. CD4 memory T cells divide poorly in response to antigen because of their cytokine profile. *Proc. Natl. Acad. Sci. USA* 105: 14521–14526.
55. Badovinac, V. P., and J. T. Harty. 2007. Manipulating the rate of memory CD8$^+$ T cell generation after acute infection. *J. Immunol.* 179: 53–63.
56. Joshi, N. S., W. Cui, A. Chandele, H. K. Lee, D. R. Urso, J. Hagman, L. Gapin, and S. M. Kaech. 2007. Inflammation directs memory precursor and short-lived effector CD8$^+$ T cell fates via the graded expression of T-bet transcription factor. *Immunity* 27: 281–295.
57. Lauvau, G., S. Vijh, P. Kong, T. Horng, K. Kerksiek, N. Serbina, R. A. Tuma, and E. G. Pamer. 2001. Priming of memory but not effector CD8 T cells by a killed bacterial vaccine. *Science* 294: 1735–1739.
58. Pham, N. L., V. P. Badovinac, and J. T. Harty. 2011. Differential role of "Signal 3" inflammatory cytokines in regulating CD8 T cell expansion and differentiation in vivo. *Front. Immunol.* 2: 4.
59. Kapina, M. A., G. S. Shepelkova, V. V. Mischenko, P. Sayles, P. Bogacheva, G. Winslow, A. S. Apt, and I. V. Lyadova. 2007. CD27^{low} CD4 T lymphocytes that accumulate in the mouse lungs during mycobacterial infection differentiate from CD27^{high} precursors in situ, produce IFN-γ, and protect the host against tuberculosis infection. *J. Immunol.* 178: 976–985.
60. Zhou, X., S. L. Bailey-Bucktrout, L. T. Jeker, C. Penaranda, M. Martínez-Llordella, M. Ashby, M. Nakayama, W. Rosenthal, and J. A. Bluestone. 2009. Instability of the transcription factor Foxp3 leads to the generation of pathogenic memory T cells in vivo. *Nat. Immunol.* 10: 1000–1007.